A new isolation method for rat intraepithelial lymphocytes

Derrick Todd, Amrik J. Singh, Dale L. Greiner, John P. Mordes, Aldo A. Rossini,
Rita Bortell *

Department of Medicine, University of Massachusetts Medical School, Worcester, MA 01655, USA

Abstract

Intraepithelial lymphocytes (IELs) play critical roles in gut immunity. In mice, $\gamma\delta$ T cells are a large component of the IEL population. In the rat, $\gamma\delta$ IELs are reportedly much less common, but technical issues suggest that previous analyses should be interpreted cautiously. The study of IELs in rats has been impeded by isolation procedures that are lengthy and complex, leading to small cell yields. For this reason, it is possible that rat IELs analyzed in previous studies have not been representative of the entire IEL compartment. We report a new method for the isolation of rat IELs that is based on the selective removal of intestinal epithelial cells under conditions that leave the basement membrane undisturbed. The method is rapid and requires neither enzymatic digestion, nor surgical removal of Peyer's patches, nor vigorous mechanical manipulation of the intestine. The yield of rat IELs using this method is 5- to 10-fold greater than that reported for other methods. Morphological and phenotypic analyses demonstrated that the purified cell population is comprised of IELs and is not contaminated with lamina propria or Peyer's patch lymphocytes. Phenotypic analysis revealed five major subsets of IELs based on differential cell surface expression of CD4, CD8, and $\alpha\beta$ T cell receptor (TcR). Among the $\alpha\beta$TcR$^-$ cells was a population of $\gamma\delta$ T cells present at levels not previously detected. The isolation of IEL sub-populations using this methodology should facilitate studies of the function of these cells in gut immunity. © 1999 Elsevier Science B.V. All rights reserved.

Keywords: Intestinal epithelial lymphocytes; Methodology; Rat; IEL; $\gamma\delta$ T cells

1. Introduction

Intestinal lymphoid cells are present in three physically and functionally distinct tissue compartments:

the lamina propria, Peyer's patches, and the intraepithelial space (Lefrançois, 1994). Analyses of cell populations in each of these compartments has been impeded by isolation methods that yield small numbers of cells and do not reproducibly prevent cross-contamination (Davies and Parrott, 1981; Mosley and Klein, 1992; Lefrançois, 1994; Ebert and Roberts, 1995; Kearsey and Stadnyk, 1996; Teitelbaum et al., 1996a,b). This has been particularly true for analyses of rat intraepithelial lymphocytes (IELs), only 5–10 million of which have typically been isolated from one animal.

Different laboratories have reported variable cell yields and IEL phenotypes (Fangmann et al., 1991a; Takimoto et al., 1992; Torres-Nagel et al., 1992; Kuhnlein et al., 1994; Gorczynski et al., 1996; Kearsey and Stadnyk, 1996; Helgeland et al., 1997; Kearsey and Stadnyk, 1997). Nonetheless, based on available purification methods, a working consensus has been reached on the phenotype of rat IELs (Takimoto et al., 1992; Sakai et al., 1994; Helgeland et al., 1996; Kearsey and Stadnyk, 1996; Teitelbaum et al., 1996a,b; Waite et al., 1996; Helgeland et al., 1997). The majority appear to be CD8$^+$ (Sakai et al., 1994; Teitelbaum et al., 1996a,b). Many of the CD8$^+$ IELs express the CD8α/α homodimer (Torres-Nagel et al., 1992). The majority of rat IELs ($>95\%$) also express the RT6 surface differentiation alloantigen at high density (Fangmann et al., 1990; Fangmann et al., 1991a,b; Colle et al., 1992; Fangmann et al., 1993; Waite et al., 1996). Most investigators have reported that $>90\%$ of IELs in euthymic rats express the $\alpha\beta$ T cell receptor (TcR) whereas $<10\%$ express the $\gamma\delta$TcR (Fangmann et al., 1991b; Torres-Nagel et al., 1992; Kuhnlein et al., 1994; Kearsey and Stadnyk, 1996; Waite et al., 1996; Helgeland et al., 1997).

The original protocols developed for IEL isolation require dissection to remove Peyer's patches, and mincing of the tissue to physically disrupt the epithelium (Davies and Parrott, 1981; Lundqvist et al., 1992; Mosley and Klein, 1992; Lefrançois, 1994). This method is limited by variable, sometimes extensive, contamination of the IEL preparation with lamina propria lymphocytes. To address this problem, the original protocols for IEL isolation (Davies and Parrott, 1981; Lefrançois, 1994) have required enzymatic digestion, chelation with agents like EDTA, panning, and/or magnetic bead separation (Davies and Parrott, 1981; Lundqvist et al., 1992; Mosley and Klein, 1992; Lefrançois, 1994). None of the modifications have proven entirely satisfactory.

An alternative method for IEL isolation everts, ligates, and distends the intestine, which is then incubated with dithioerythritol (DTE) and subjected to repeated rigorous vortexing (Mayrhofer and Whately, 1983). Using discontinuous Percoll gradient centrifugation, yields of $\sim 5 \times 10^6$ IELs/rat that are $\sim 90\%$ pure have been obtained (Kearsey and Stadnyk, 1996). Contamination of this IEL preparation with lymphocytes from lamina propria and Peyer's patches is minimal. The low cell yield, however, makes it uncertain that phenotypic and functional characteristics of IELs prepared in this way are representative of the entire, much larger, IEL compartment (Mayrhofer and Whately, 1983; Kearsey and Stadnyk, 1996).

To address these issues, we have developed an efficient new technique for the rapid isolation of large numbers of highly purified rat IELs. The technique is based in part on the susceptibility of intestinal epithelial cells to hypoxic conditions that leave the basement membrane relatively undisturbed. The sloughed epithelium carries with it the IELs, effectively dissecting away the lamina propria and Peyer's patches. IELs prepared in this way are high in yield and purity. They contain five major subsets, including a population of $\gamma\delta$ T cells present at levels much higher than previously described.

2. Materials and methods

2.1. Animals

Ten- to 16-week old Wistar Furth (WF) (RT1^u, RT6^b), BN (RT1^n, RT6^b), DA (RT1^a, RT6^b), and F344 (RT1^{lv}, RT6^b) rats were obtained from Harlan Sprague–Dawley (Indianapolis, IN). DR-BB (RT1^u, RT6^a) and PVG.RT1^u (RT1^u, RT6^a) rats were obtained from BMR (Worcester, MA). Except where noted, all analyses were performed using 10- to 12-week old WF rats.

Rat tissue donors were killed in an atmosphere of 100% CO_2. Animals in this study were continuously monitored for infection and were serologically free of Sendai virus, pneumonia virus of mice, sialodacryoadenitis virus, rat corona virus, Kilham rat virus, H1 (Toolan's virus), GD7, Reo-3, *Mycoplasma pulmonis*, lymphocytic choriomeningitis virus, mouse adenovirus, Hantaan virus, and *encephalitozoon cuniculi*. Animals of either sex were studied. All animals were maintained in accordance with recommendations in the *Guide for the Care and Use of Laboratory Animals* (Institute of Laboratory Animal Resources, National Research Council, National Academy of Sciences, 1996) and the guidelines of the Institutional Animal Care and Use Com-

mittee (IACUC) of the University of Massachusetts Medical Center.

2.2. Antibodies

The hybridoma cell line secreting the 6A5 anti-RT6.2 (rat IgG1) is maintained in our laboratory. Monoclonal antibodies (mAbs) directed against $\alpha\beta$TcR (clone R7.3), CD8α (clone OX-8), CD8β (clone 341), CD4 (clone OX-35), B220 (CD45R, clone HIS24), CD25 (IL-2 receptor α-chain, clone OX-39), CD2 (LFA, clone OX-34), CD3 (clone G4.18), CD5 (clone OX-19), CD28 (clone JJ-319), CD45RC (OX-22), NKR-P1A (10/78), anti-$\gamma\delta$TcR (clones V45 and V65), and the appropriate isotype controls for each mAb were obtained from PharMingen (San Diego, CA).

2.3. Flow microfluorometry

Single-, two-, and three-color flow cytometric analyses were performed as previously described (Zadeh et al., 1996; Iwakoshi et al., 1998). Briefly, 1×10^6 viable lymph node cells or IELs were reacted with a mixture of fluorescein isothiocyanate (FITC), biotin, and/or phycoerythrin (PE)-conjugated mAbs for 20 min at 4°C. All IEL analyses were performed after nylon wool or Percoll-density gradient purification to remove the large number of contaminating dead epithelial cells. Cells were then washed, reacted with Cy-Chrome®-conjugated streptavidin (PharMingen) to visualize biotinylated mAbs, washed again, and fixed with 1% paraformaldehyde. FITC-, biotin- and PE-conjugated isotype control immunoglobulins (PharMingen) were used for all analyses. Cells were analyzed using a FACScan® instrument (Becton Dickinson, Sunnyvale, CA). Lymphoid cells were identified by their forward and side light-scatter profiles and the detection of RT6, $\alpha\beta$TcR, or $\gamma\delta$TcR staining. The composite phenotypes of lymphoid cell subsets for up to four antigenic markers were determined by combining the results of multiple two- and three-color analyses of replicate samples of lymphocytes, each incubated with a different combination of antibodies.

To characterize the sub-population containing NKR-P1$^+$ cells using three color flow cytometry, we exploited the unique staining patterns of CD8α,

CD4, and $\alpha\beta$TcR on IELs. Because < 1% of IELs express the CD8α^-CD4$^-\alpha\beta$TcR$^+$ phenotype, further analysis of CD8α^-CD4$^-\alpha\beta$TcR$^-$ IELs was possible by labeling with CD8α and CD4, selecting the CD8α^-CD4$^-$ IEL subset, and performing three color analysis using a third fluorochrome.

To characterize the CD8$^+$CD4$^-\alpha\beta$TcR$^-$ subpopulation, we again exploited the unique staining patterns of CD8α, CD4, and $\alpha\beta$TcR on IELs. Because CD8α^+CD4$^+\alpha\beta$TcR$^-$ IELs comprise < 1% of IELs, it was possible to stain for CD8α and $\alpha\beta$TcR, select the CD8$\alpha^+\alpha\beta$TcR$^-$ cells, and examine this population using a third fluorochrome, e.g., anti-$\gamma\delta$TcR using the V65 mAb. IELs expressing the CD8α^+CD4$^-\alpha\beta$TcR$^-$ phenotype were shown to be $\gamma\delta$TcR$^+$ (see Fig. 6). Sub-populations of cells with this phenotype were therefore identifiable by dual labeling for V65 and a second fluorochrome.

Strategies for analyzing the remaining three $\alpha\beta$TcR$^+$ populations were as follows. Because CD8α^-CD4$^+\alpha\beta$TcR$^-$ cells comprise < 1% of total IELs, CD8α^-CD4$^+\alpha\beta$TcR$^+$ IELs could be analyzed by staining for CD8α and CD4, selecting for CD8α^-CD4$^+$ cells, and examining this population using a third fluorochrome. Because CD8α^+CD4$^+$ $\alpha\beta$TcR$^-$ cells comprise < 1% of total IELs, D8α^+CD4$^+\alpha\beta$TcR$^+$ IELs could be analyzed by staining for CD8α and CD4, selecting for CD8α^+CD4$^+$ cells, and examining this population using a third fluorochrome. Finally, because CD8α^-CD4$^-\alpha\beta$TcR$^+$ cells comprise < 1% of total IELs, CD8α^+CD4$^-\alpha\beta$TcR$^+$ IELs could be analyzed by staining for CD4 and $\alpha\beta$TcR, selecting for CD4$^-\alpha\beta$TcR$^+$ cells, and examining this population using a third fluorochrome.

2.4. Intraepithelial lymphocyte preparation

To prepare IELs, the proximal 3–4 cm of intestine including the duodenum was first dissected free of the pancreas, and the bowel was transected at the level of the pyloric sphincter. The remainder of the small intestine was dissected free of omentum by gentle blunt dissection, transected 1 cm proximal to the ileo-cecal junction, and removed en bloc. Care was taken to avoid perforation of the intestine during dissection. Intestinal contents were removed by gently flushing the lumen with 50 ml of cold (4°C)

RPMI 1640 over a 3-min period using a 1-mm gavage tube inserted into the proximal lumen. Flushing to remove fecal material was performed gently, at low pressure, and without squeezing the bowel, so as not to perforate the bowel wall or disturb the epithelial mucus coating that contains large numbers of lymphoid cells. The intestine was then immersed in cold RPMI 1640 and incubated on ice for 60–120 min. IELs were recovered in a two step procedure.

Step 1: After cold incubation, the intestinal lumen was flushed at low pressure (over several minutes) with 10 ml of medium consisting of HEPES-buffered HBSS containing 1 mM DTE and 10% Fetalclone® I (a defined neonatal bovine serum, HyClone, Logan, UT) at 37°C. The lumenal eluate was saved.

Step 2: The weakly adherent epithelial cells and mucus coating remaining in the intestine were then squeezed out by manual compression as follows. The proximal end of the intestine was grasped between thumb and index finger and suspended vertically over a polystyrene container. The thumb and index finger of the other hand were then slid along the entire length of the gut, compressing it from duodenum to distal ileum to extrude mucus and cellular contents. Care was taken to avoid tearing the tissue.

The specimen was subjected to a total of five cycles of flushing (Step 1) and squeezing (Step 2) to extrude all intra-lumenal contents. The contents of all five 10 ml flushes and extrusions were combined in one 50 ml polystyrene test tube. The tube was then gently swirled to suspend all cells. Clumps of material present in the dispersed sediment were allowed to settle for 10 min. The supernatant containing single dispersed epithelial cells and IELs was then removed by pipetting into a second tube and centrifuged at $350 \times G$ for 5 min. The resulting pellet, containing IELs, erythrocytes, and epithelial cells, was then recovered and subjected to either nylon wool or density gradient centrifugation for further purification.

The viability of IELs prepared in this way was assessed immediately after their recovery by the method of Trypan blue exclusion. We observed that > 95% of the lymphoid cells were viable. In contrast, > 90% of the epithelial cells in the freshly isolated population failed to exclude the dye.

2.5. Lymph node cell preparation

Cervical and mesenteric lymph nodes were removed and single cell suspensions were prepared by gentle extrusion through stainless steel sieves into cold medium (Zadeh et al., 1996). Intestine was removed prior to the recovery of mesenteric lymph nodes.

2.6. Nylon wool purification of IELs

Nylon wool purification of IEL suspensions was performed as described previously (Lefrançois, 1994). Briefly, pelleted cells were suspended in 10 ml cold RPMI containing 5% Fetalclone® I, and passed through a loosely packed nylon wool column at the rate of 1 drop every 1–2 s. The column was washed with cold medium containing 5% Fetalclone® I. The number of viable cells with lymphoid morphology was quantified using a hemocytometer and the method of Trypan blue exclusion.

2.7. Discontinuous Percoll density gradient purification of IELs

A two step discontinuous Percoll density gradient centrifugation procedure was used in some experi-

---

Fig. 1. Histological analysis of gut and isolated cell populations at various stages of IEL preparation. (A) Normal 16-week old WF rat jejunum showing epithelium closely apposed to lamina propria ($\times 10$). (B) Appearance of rat jejunum after incubation for 120 min at 4°C. The epithelial layer is delaminating from the basement membrane along cleavage planes (arrows) with no disruption of the lamina propria ($\times 10$). (C and D) Appearance of the lumenal surface of the jejunum after completion of the five cycles of intestinal perfusion and extrusion. Panel C shows that most epithelial cells are absent from the villi, although some remain ($\times 20$). The arrow identifies a point of demarcation between residual epithelium and denuded, but intact, lamina propria from which the epithelium has sloughed. Panel D shows additional areas of lamina propria (arrows) and an intact Peyer's patch (asterisk); both are denuded of gut epithelium ($\times 20$). (E) H&E stained paraffin-embedded sample of the cells present in the crude lumenal perfusate of the intestine. Small round cells consistent with lymphocytes are abundant, as are larger epithelial cells ($\times 20$). (F) Giemsa-stained cytospin sample of Percoll density gradient-purified IELs. Larger cells containing granules are indicated by arrows ($\times 60$).

ments (Kearsey and Stadnyk, 1996). Briefly, pelleted cells were re-suspended in 35 ml RPMI containing 5% Fetalclone® I at room temperature; 15 ml of

Percoll was then added to generate a 30% Percoll solution. The cell suspension was centrifuged at $350 \times G$ for 15 min at room temperature. Non-viable
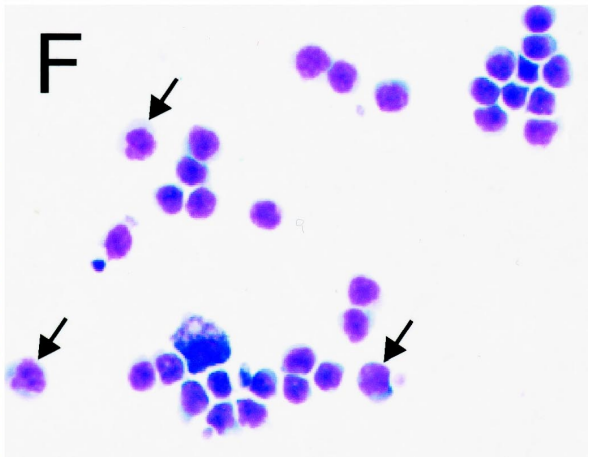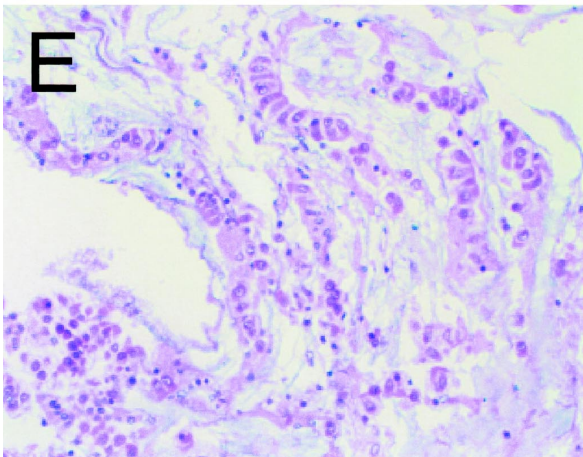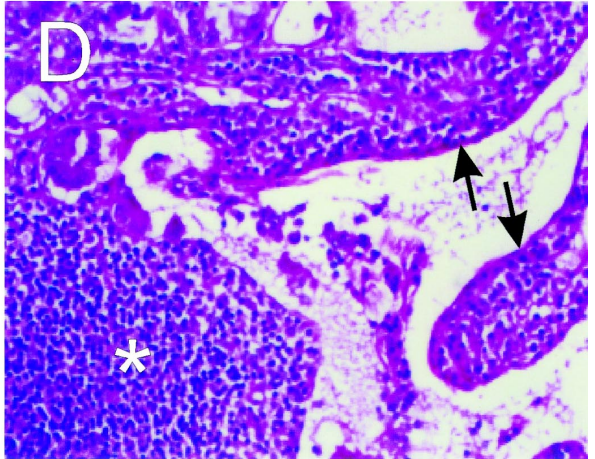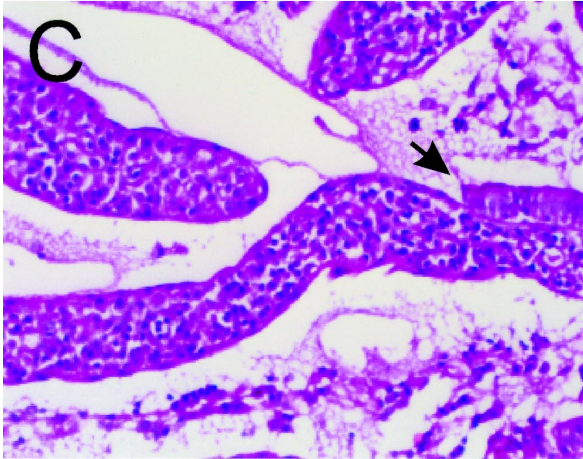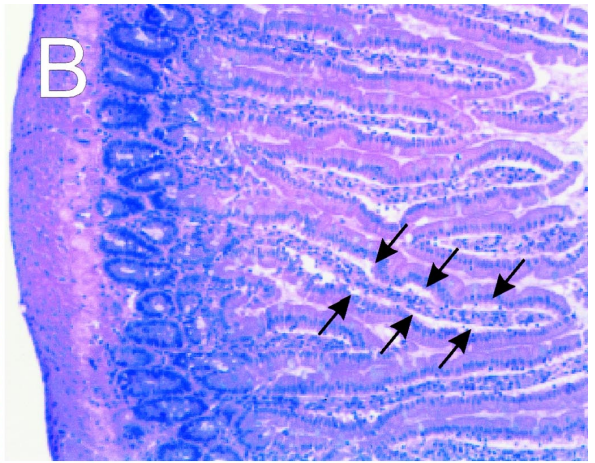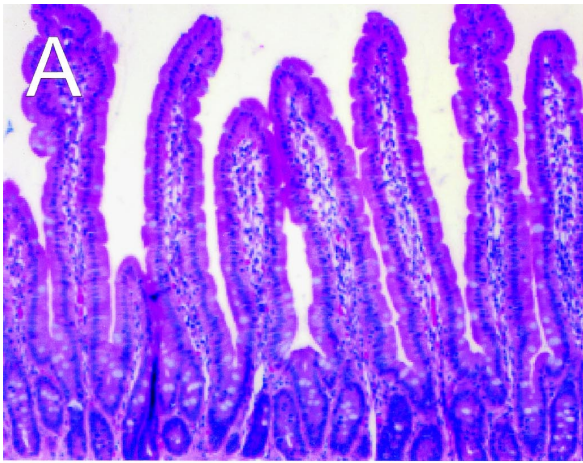
epithelial cells were excluded from the 30% Percoll solution, whereas erythrocytes, lymphocytes, and viable epithelial cells localized to the pellet. The cell pellet was suspended in 15 ml of a 45% Percoll solution. A second 75% Percoll solution was layered under the 45% solution, and the discontinuous Percoll gradient was then centrifuged at $350 \times G$ for 30 min. Viable epithelial cells were recovered from the supernatant at the 45% interface. Red blood cells and debris migrated into the layer of 75% Percoll. Viable IELs were collected from the interface between the 45% and 75% Percoll layers. The number of viable cells that excluded Trypan blue was quantified using a hemocytometer and was $> 95\%$ in all cases.

2.8. Histology

Samples of 16-week old WF rat intestine for histological analysis were taken at three different stages of the IEL isolation procedure. The first was obtained immediately after the animal was killed in an atmosphere of 100% CO_2. The second was recovered after incubation at 4°C, but before perfusion with medium at 37°C. The third was recovered after five perfusions and extrusions. Specimens were immediately fixed in 10% buffered formalin or Bouin's fixative. Paraffin-embedded tissue sections of all samples were stained with hematoxylin and eosin (H&E) and examined by light microscopy. Samples of the extruded intra-lumenal contents were embedded in paraffin, stained with H&E, and examined by light microscopy. Cytospin-prepared slides of Percoll-purified IEL were prepared and stained with Giemsa for analysis of purity.

3. Results

3.1. Intestinal morphology before and after IEL isolation: Peyer's patches and lamina propria remain intact

Samples of WF intestine were taken at different stages of the isolation procedure and examined by

Table 1
Yield of purified WF rat IELs

| Purification technique	Percentage of cells in lymphoid gate	Lymphoid cells recovered ($\times 10^6$)
Nylon wool	79.9 ± 8.9 ($N = 7$)	33.6 ± 8.1 ($N = 7$)
Percoll density gradient centrifugation	97.4	21.8 ± 3.6 ($N = 4$)

The total number of viable mononuclear cells present in the purified preparations was determined using a hemocytometer. Contaminating large epithelial cells (see Fig. 1) were excluded. The percentage of lymphocytes present in the purified cell populations was measured by flow cytometry on the basis of forward- and side-scatter. The number of individual samples tested is shown in parenthesis except in the case of the percentage of lymphocytes present in Percoll-purified cells. In this instance, the percentage was measured on a single pool of IELs from four animals. Data are expressed as the mean $\pm$ s.d.

light microscopy. Fig. 1, panel A shows the anatomy of normal 16-week old WF rat jejunum. Panels B, C, and D show progressive changes in gut morphology during processing for the recovery of IELs. They document delamination (panel B) and removal (panels C and D) of the intestinal epithelium from the basement membrane. Panels C and D also document the presence of intact lamina propria and Peyer's patches in the residual processed intestine. Panel E shows the morphology of cells present in the unpurified lumenal washing after five cycles of extrusion. Numerous mononuclear cells are present together with epithelial cells.

3.2. Yield and purity of IEL preparations

IEL yield and purity were measured after nylon wool or Percoll purification of the lumenal washings. Nylon wool purification resulted in higher yields of IELs but slightly lower purity than did Percoll purification.

Fig. 2. Flow cytometric profiles based on light scatter of WF rat IELs and peripheral lymph node cells. Forward scatter (horizontal axis) is plotted against side scatter (vertical axis). Shown are representative profiles of nylon wool-purified WF rat IELs (top panel), Percoll gradient purified IELs (middle panel), and peripheral lymph node cells (bottom panel). The gate was established on the peripheral lymph node cell population. Comparable results were obtained in four to seven individual animals (Table 1).
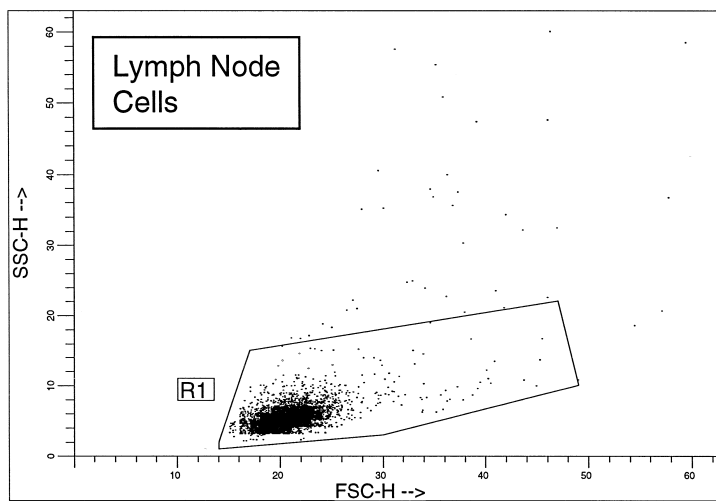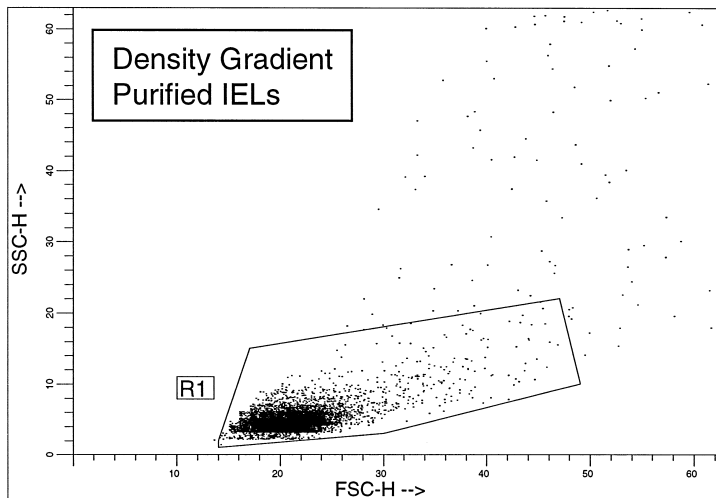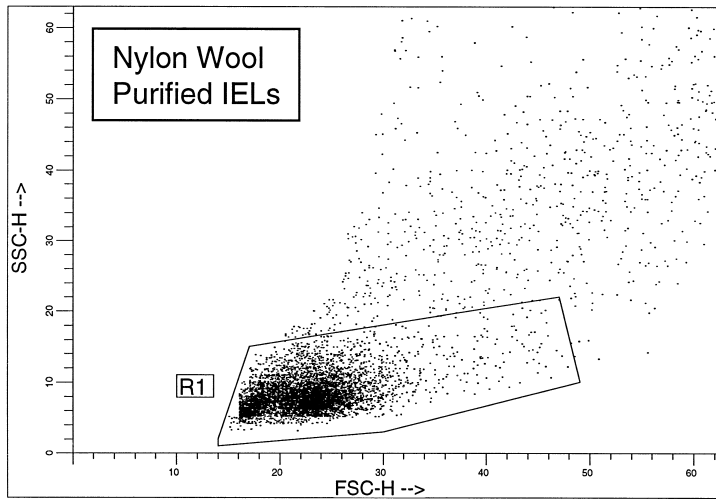
3.2.1. Nylon wool purification

Yields following nylon wool purification averaged 33.6×10^6 viable IELs/rat (range 27.2 to 48.0 $\times 10^6$, $N = 7$, Table 1). Flow cytometric analysis of the purified cells based on forward- and side-scatter demonstrated that lymphocytes comprised $\sim 80\%$ of total cells (Table 1 and Fig. 2, panel A).

3.2.2. Discontinuous Percoll gradient purification

Compared with nylon wool purification, discontinuous Percoll density gradient centrifugation resulted in lower IEL recovery but greater purity. Average yield was 21.8×10^6 viable IELs/rat (range 17.8 to 26.6×10^6, $N = 4$, Table 1). Flow cytometric analysis revealed that $> 97\%$ of cells were lymphocytes (Fig. 2, panel B). Analysis of the light-scattering properties of both the nylon wool and Percoll-purified lymphoid cells revealed that they were slightly larger than peripheral lymph node cells (Fig. 2, panel C). Morphological analyses of Percoll-purified cells revealed large numbers of mononuclear cells similar in appearance to unfractionated lymph node cells (Fig. 1, panel F). Some of these mononuclear cells are large and appear to contain granules.

3.3. Phenotype of purified IELs

The phenotype of purified intestinal lymphocyte populations was determined by flow cytometry. In preliminary studies, it was determined that the phenotypes of the intestinal lymphoid cells purified by nylon wool and by Percoll density gradient centrifugation were qualitatively similar (data not shown). The phenotypic analyses presented below were performed on nylon wool-purified cells.

3.4. Isolated cells are predominantly $RT6^+ CD8\alpha^+ B220^-$

The phenotype of cells isolated using our methodology displayed the consensus phenotype of IELs (Takimoto et al., 1992; Sakai et al., 1994; Helgeland et al., 1996; Kearsey and Stadnyk, 1996; Teitelbaum et al., 1996a,b; Waite et al., 1996; Helgeland et al., 1997). Consistent with previous reports (Fangmann
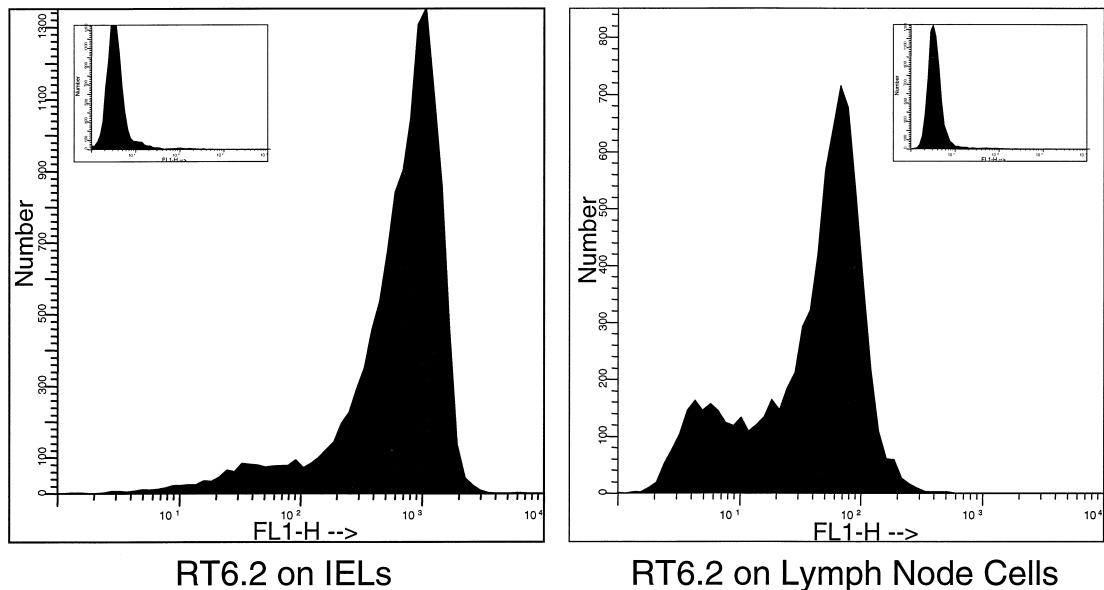
Fig. 3. Flow cytometric analysis of RT6 expression on WF rat IELs and peripheral lymph node cells. Fluorescence intensity (horizontal axis) is plotted against cell number (vertical axis). Shown are representative profiles of RT6.2 expression on lymphocyte-gated nylon wool purified WF rat IELs (left panel) and WF rat cervical lymph node cells (right panel). The insets show fluorescence profiles of the same cell populations reacted with FITC-conjugated isotype control immunoglobulin. Comparable results were obtained in three to six individual animals.

Table 2
Expression of CD4, CD8α, and αβTcR defines five sub-populations of WF rat IELs

Phenotype	CD8α$^+$CD4$^+$ αβTcR$^+$	CD8α$^+$CD4$^-$ αβTcR$^+$	CD8α$^+$CD4$^-$ αβTcR$^-$	CD8α$^-$CD4$^+$ αβTcR$^+$	CD8α$^-$CD4$^-$ αβTcR$^-$
Percent of IELs	5.7 ± 2.8	31.8 ± 3.3	24.2 ± 4.1	8.6 ± 1.1	30.5 ± 5.1

Nylon wool-purified WF rat IELs were analyzed by three-color flow cytometry for the expression of CD4, CD8α and αβTcR (see Section 2). Five of the eight possible combinations of these markers comprised > 99% of all IELs. The percentage of CD8α$^+$CD4$^+$αβTcR$^-$, CD8α$^-$CD4$^+$αβTcR$^-$, and CD8α$^-$CD4$^-$αβTcR$^+$ IELs was < 1% of total cells. Each data point represents the mean ± s.d. of six individual samples.

et al., 1990, 1991a,b; Waite et al., 1996), the percentage of RT6$^+$ cells was very high (92 ± 3%, Fig. 3). More than half (62 ± 5%) of the IELs expressed CD8α, and ~ 60% of the CD8α$^+$ cells were CD8α$^+$β$^-$. Less than 5% of the IEL population was B220$^+$ (i.e., CD45R$^+$ B cells).

Consistent with previous reports (Fangmann et al., 1991a,b; Waite et al., 1996), the RT6$^+$ cells in the IEL population (Fig. 3, panel A) expressed RT6 at a higher surface density than did lymph node cells (Fig. 3, panel B). Taken together, these phenotypic and morphological results confirm that our methodology selectively isolates IELs while excluding contaminating lamina propria and Peyer's patch lymphocytes, a large number of which express B220.

3.5. Differential expression of CD4, CD8, and αβTcR classifies rat IELs into five major sub-populations

Differential expression of CD8α, CD4, and αβTcR expression segregated > 99% of the total
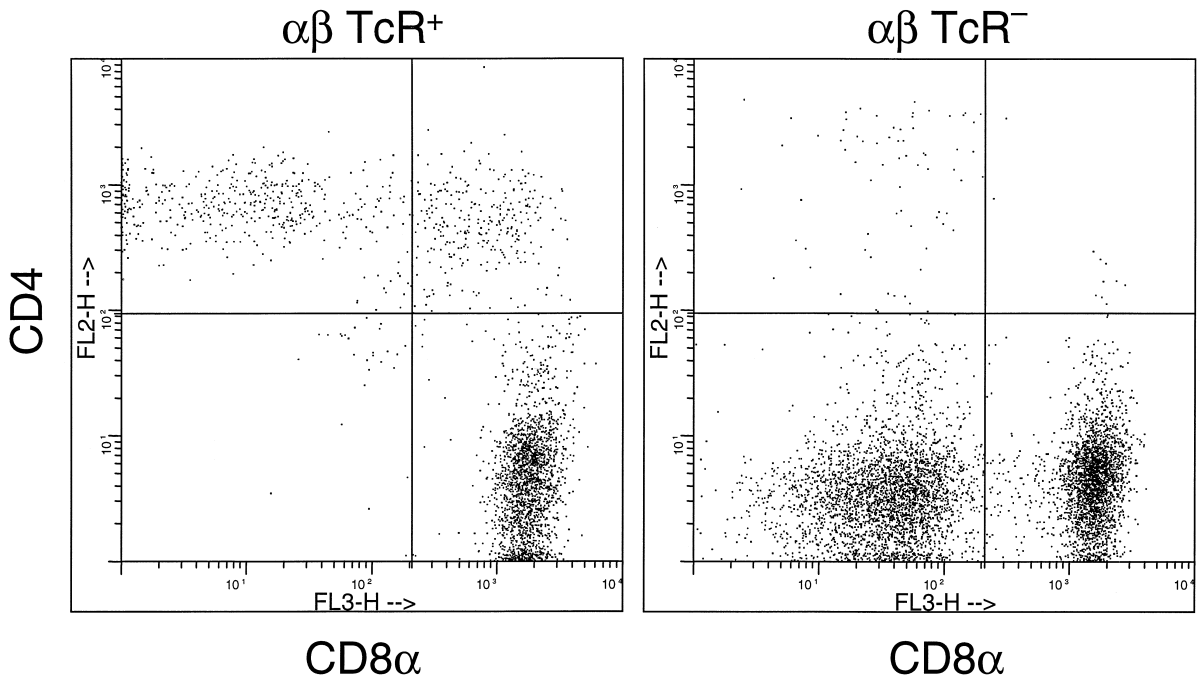
Fig. 4. Three color flow cytometric analysis of the expression of CD4, CD8, and αβTcR by WF rat IELs. The expression of CD4 (vertical axis) and CD8 (horizontal axis) was determined on lymphocyte-gated, nylon wool purified αβTcR$^+$ (left panel) and αβTcR$^-$ IELs (right panel). Shown is a single representative analysis of the five major IEL sub-populations defined by these three surface markers. Comparable results were obtained in six individual analyses (Table 2).
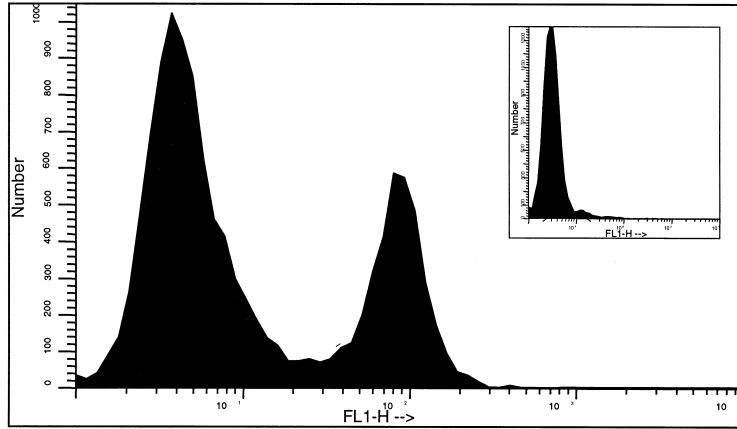
Total IELs Stained for NKR-P1
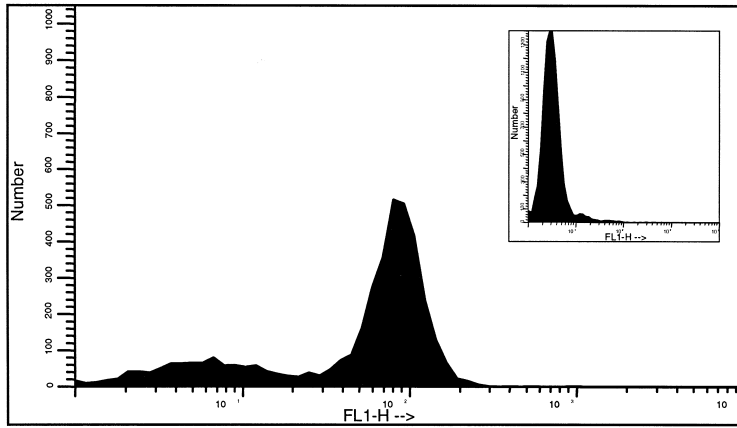
CD4⁻CD8⁻ IELs Stained for NKR-P1
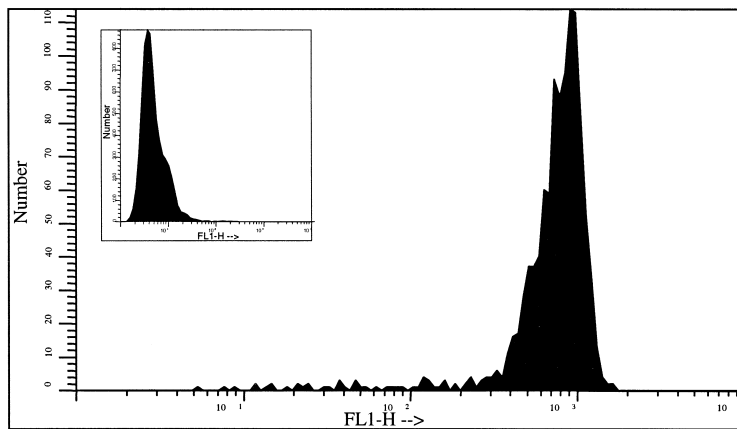
NKR-P1⁺ Cells Stained for RT6.2

Total IELs Stained for γδ TcR   αβ TcR⁻ CD8⁺ IELs Stained for γδ TcR
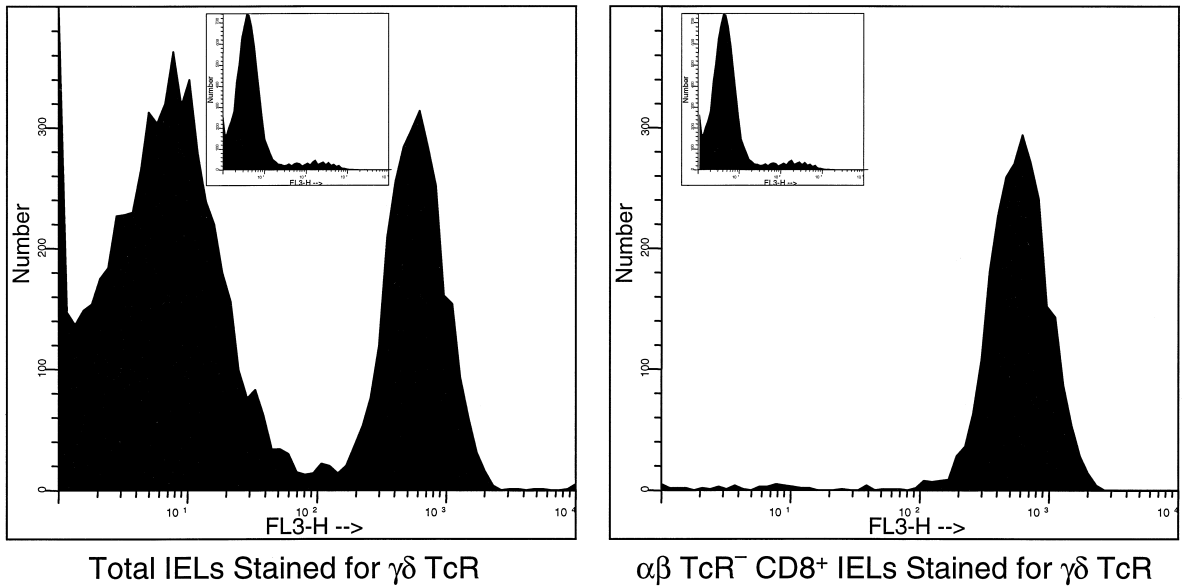
Fig. 6. Flow cytometric analysis of $\gamma\delta$TcR expression on WF rat IELs. Fluorescence intensity (horizontal axis) is plotted against cell number (vertical axis). Cells were reacted with the V65 mAb to identify $\gamma\delta$TcR$^+$ cells. Shown are representative profiles of $\gamma\delta$TcR expression on lymphocyte-gated nylon wool purified total WF rat IELs (left panel) and on CD8$^+\alpha\beta$TcR$^-$ cells (right panel). The insets show fluorescence profiles of the same cell populations reacted with Cy-Chrome®-conjugated isotype control immunoglobulin. Comparable results were obtained in six individual animals.

population of purified IELs into one of five major non-overlapping subsets (Table 2, Fig. 4). As expected on the basis of previous reports (Takimoto et al., 1992; Torres-Nagel et al., 1992; Sakai et al., 1994; Helgeland et al., 1996; Teitelbaum et al., 1996a,b; Helgeland et al., 1997), CD8α^+CD4$^-$ $\alpha\beta$TcR$^+$ cells comprised a major sub-population (32%) of IELs (Fig. 4, left panel). CD8α^-CD4$^+$ $\alpha\beta$TcR$^+$ and CD8α^+CD4$^+\alpha\beta$TcR$^+$ cells comprised $\sim$9% and $\sim$6% of IELs, respectively. Surprisingly, CD8α^-CD4$^-\alpha\beta$TcR$^-$ and CD8α^+ CD4$^-\alpha\beta$TcR$^-$ cells comprised $\sim$30% and $\sim$25% of the purified IEL population, respectively (Fig. 4, right panel). The three remaining permutations of these three surface antigens (CD8α^+CD4$^+\alpha\beta$TcR$^-$, CD8α^-CD4$^+\alpha\beta$TcR$^-$, and CD8α^-CD4$^-\alpha\beta$TcR$^+$)

together were observed on less than 1% of the total population (Fig. 4, Table 2).

3.6. Natural killer (NK) cells and $\gamma\delta$TcR$^+$ T cells are abundant in the two $\alpha\beta$TcR$^-$ rat IEL populations

Unexpectedly, $23.7 \pm 4.2\%$ ($N = 6$) of all IELs were observed to express the NKR-P1 antigen characteristic of NK cells and NK T cells (Fig. 5, top panel). To determine if any of these were NK T cells, we characterized further each of the five IEL sub-populations. We observed that $64.1 \pm 9.1\%$ ($N = 6$) of CD8α^-CD4$^-$ IELs ($\sim$99% of which are $\alpha\beta$TcR$^-$, see above) were NKR-P1$^+$, accounting for most ($87.1 \pm 6.5\%$) of the NKR-P1 IEL population

Fig. 5. Flow cytometric analysis of NKR-P1 and RT6.2 expression on WF rat IELs. Fluorescence intensity (horizontal axis) is plotted against cell number (vertical axis). Shown are representative profiles of NKR-P1 expression on lymphocyte-gated nylon wool purified WF rat IELs (top panel), NKR-P1 expression on CD8$^-$CD4$^-$ cells (middle panel) and RT6.2 expression on NKR-P1$^+$ IELs (bottom panel). The insets show fluorescence profiles of the same cell populations reacted with FITC-conjugated isotype control immunoglobulin. Comparable results were obtained in six individual animals.

Table 3
Phenotypic characteristics of the five major sub-populations of WF rat IELs

	$CD8\alpha^+ CD4^+$ ($\alpha\beta TcR^+$)	$CD4^- \alpha\beta TcR^+$ ($CD8\alpha^+$)	$\gamma\delta TcR^+$ ($CD8\alpha^+ CD4^-$)	$CD8\alpha^- CD4^+$ ($\alpha\beta TcR^+$)	$CD8\alpha^- CD4^-$ ($\alpha\beta TcR^-$)	Total IELs	$CD4^+$ lymph node cells
RT6.2	96.3 ± 3.2	98.9 ± 0.5	99.3 ± 0.3	78.4 ± 3.3	77.9 ± 10.2	91.6 ± 2.7	83.9 ± 0.6
CD2	14.8 ± 9.9	2.3 ± 0.5	2.6 ± 1.6	59.4 ± 6.0	1.1 ± 0.2	7.2 ± 0.9	99.2 ± 0.1
CD3	99.9 ± 0.2	99.9	99.9	93.4 ± 1.7	22.3 ± 14.0	73.7 ± 4.8	99.5 ± 0.1
CD5	95.1 ± 3.8	58.0 ± 9.3	5.7 ± 3.0	94.2 ± 1.8	5.0 ± 4.2	33.7 ± 8.7	98.1 ± 0.2
CD25	78.2 ± 7.9	90.3 ± 4.3	98.6 ± 0.4	79.3 ± 2.0	72.2 ± 13.6	84.5 ± 5.4	8.6 ± 0.9
CD28	71.5 ± 11.0	15.6 ± 2.3	5.0 ± 2.2	86.5 ± 2.5	2.3 ± 0.5	16.5 ± 2.0	97.3 ± 0.5
CD45RC[intermediate]	13.1 ± 10.0	34.4 ± 9.4	7.6 ± 2.5	8.8 ± 1.3	4.5 ± 2.5	13.8 ± 3.1	56.4 ± 2.1

Subset percentages for each major IEL subset, total IELs, and peripheral lymph node cells. Each of the five nylon wool-purified WF rat IEL populations defined in Table 2 on the basis of differential expression of $CD8\alpha$, CD4, and $\alpha\beta TcR$ was further analyzed for expression of the seven additional phenotypic markers listed in the leftmost column. Phenotypes shown in parentheses are inferred, not directly determined (see Sections 2 and 2.3). For comparison, the expression of these seven additional phenotypic markers was also analyzed using samples of total IELs and $CD4^+$ peripheral T cells. Each IEL and lymph node data point represents the mean percentage $\pm$ s.d. measured in six and three individual samples, respectively. The percentages of $CD4^+$ peripheral lymph node cells expressing each of these seven phenotypes were essentially identical to the percentages expressed by $CD8\alpha^+$ peripheral lymph node cells (data not shown).

(Fig. 5, middle panel). This phenotype identifies them as NK cells. In addition, we observed that the majority of NKR-P1$^+$ NK IELs express high levels of cell surface RT6 (Fig. 5, bottom panel). In dual label analyses, we observed that $\sim 8\%$ of the IELs co-expressed CD3 and NKR-P1, a phenotype that is consistent with that of NK T cells. Additional dual-label analyses using anti-CD8α and anti-CD3 antibodies revealed that $< 1.5\%$ of the IEL population is CD3$^-$CD8α^+, making it unlikely that the NK IEL population is significantly contaminated with CD8$^+$ peripheral NK cells.

A second surprising observation was that $24.4 \pm 3.3\%$ ($N = 6$) of all IELs were labeled by the V65 anti-$\gamma\delta$TcR mAb (Fig. 6, left panel). Because $\alpha\beta$TcR and $\gamma\delta$TcR are not co-expressed on T cells, and because the data above indicate that the great majority of CD8$^-$CD4$^-\alpha\beta$TcR$^-$ cells are NK cells, we next tested the hypothesis that the $\gamma\delta$TcR$^+$ cells would be found in the CD8$^+$CD4$^-$ $\alpha\beta$TcR$^-$ sub-population. We observed that $94.9 \pm 1.5\%$ of the CD8α^+ $\alpha\beta$TcR$^-$ population was $\gamma\delta$TcR$^+$ (Fig. 6, right panel), accounting in turn for 95% of all $\gamma\delta$TcR$^+$ IELs.

To confirm that this high percentage of $\gamma\delta$TcR$^+$ IELs was not specific to the WF rat, we also measured the number of CD8$^+\alpha\beta$TcR$^-$ IELs isolated in the same way from rats of five additional strains. The number of CD8$^+\alpha\beta$TcR$^-$ IELs in these strains was $19.0 \pm 6.3\%$ (range 10.0% to 27.8%, $N = 9$ samples). This percentage is comparable to that observed in WF rats of the same age (Table 2).

We also measured for the percentage of $\gamma\delta$TcR$^+$ IELs using the V45 mAb that is known to react with a subset of $\gamma\delta$TcR$^+$ cells (Kuhnlein et al., 1996). We observed that V45 labeled $2.0 \pm 0.4\%$ ($N = 6$) of total IELs and $7.1 \pm 1.1\%$ ($N = 6$) of V65$^+$ IELs (data not shown).

3.7. Phenotypic characteristics of the five major IEL subsets

Each the five IEL populations defined on the basis of differential expression of CD8α, CD4, and $\alpha\beta$TcR was further analyzed for expression of seven additional phenotypic markers (Table 3). To do so, we again exploited the unique staining patterns of CD8α, CD4, and $\alpha\beta$TcR on IELs (see Section 2).

The expression of CD2, CD3, CD5, CD25, CD28, CD45RC^{intermediate}, and RT6.2 on each of the five major sub-populations of WF IELs is shown in Table 3. Consistent with previous reports (Fangmann et al., 1991a,b; Waite et al., 1996), RT6 was expressed uniformly and at high density on four of the five IEL subsets. In contrast, its expression on the CD4$^+$CD8$^-$ IEL subset was heterogeneous and at low density, a pattern also observed on CD4$^+$ peripheral T cells (Crisá et al., 1990).

Consistent with previous reports (Fangmann et al., 1991b), we observed that, unlike peripheral T cells, few IELs expressed CD2. Those cells that were CD2$^+$ were found in the CD4$^+$CD8$^-$ sub-population. Only one sub-population failed to express CD3; this was the CD4$^-$CD8$^-$ subset, which also failed to express $\alpha\beta$TcR or $\gamma\delta$TcR and, as documented above, was comprised predominantly of NK cells.

Most IELs, including $\gamma\delta$TcR$^+$ IELs, appeared to be in an activated state as evidenced by their uniform expression of CD25. Surprisingly, despite the expression of CD25, many IELs, including those in the $\gamma\delta$TcR$^+$ subset, did not express CD28. CD28 is a co-stimulatory molecule expressed constitutively on most peripheral T cells and at high levels on activated T cells.

Most subsets of IELs contained low percentages of CD45RC^{intermediate} cells. Only the CD4$^-\alpha\beta$TcR$^+$ subset contained levels of CD45RC^{intermediate} cells (34%) that approached those observed in peripheral CD4$^+$ T cell populations (56.4%, Table 3). The percentages of CD4$^+$ peripheral lymph node cells expressing each of these seven phenotypes was essentially identical to the percentages expressed by CD8$^+$ peripheral lymph node cells (data not shown).

The percentage of CD5$^+$ cells varied among the different IEL subsets. CD5 was expressed by a very low percentage of $\gamma\delta$TcR$^+$ and CD8$^-$CD4$^-$ IELs, approximately half of CD4$^-\alpha\beta$TcR$^+$ IELs, and the great majority of CD8α^+CD4$^+$ and CD8α^-CD4$^+$ IELs.

4. Discussion

The analysis of rat IEL populations recovered using our new isolation procedure has generated three principal findings. First, the method leads to

the recovery of 5- to 10-fold more IELs than are recovered using older methods (Fangmann et al., 1991b; Teitelbaum et al., 1995; Kearsey and Stadnyk, 1996; Teitelbaum et al., 1996a,b; Kearsey and Stadnyk, 1997). The method is reproducible and yields lymphoid cell preparations that are of high purity and exhibit the consensus morphologic and phenotypic characteristics of true IELs. Second, analysis of rat IELs prepared using the new method revealed the presence of $\gamma\delta$ T cells at levels not previously appreciated. In general, $\sim 25\%$ of the cells in each preparation were $\gamma\delta TcR^+$ cells. Third, three-color microfluorometric analysis classified $>$ 99% of the rat IELs into one of five major sub-populations based on their expression of TcR, CD4 and CD8. Surprisingly, one of these sub-populations was comprised predominantly of NK cells.

4.1. Isolation technology

The new method that we describe is rapid and reproducibly yields large numbers of viable IELs. The technique is based on the propensity of intestinal epithelial cells to slough off the gut basement membrane after exposure to cold and hypoxic culture conditions that leave the basement membrane relatively undisturbed. The sloughed epithelium carries with it the IEL population, effectively dissecting away the lamina propria and Peyer's patches.

The procedure yields a population of cells that fulfill three criteria that define a successful IEL purification process. First, the lamina propria and Peyer's patches remain intact throughout the isolation procedure. Second, the morphology and light-scattering properties of the recovered cells are those of intestinal epithelial lymphocytes. Finally, the phenotype of the purified cells is consistent with that of an IEL population (Fangmann et al., 1990; Kearsey and Stadnyk, 1996).

The methodology is noteworthy for two additional reasons. The first is its technical simplicity. It requires no special reagents or equipment, nor does it require extensive or vigorous mechanical disturbance of the intestine. It takes only 2–3 h, yet reproducibly generates large numbers of pure IELs.

Second, and more importantly, the methodology appears to generate cell populations that are more representative of the entire IEL compartment than are populations generated by older methods. We believe this to be the case because our method overcomes two obstacles that have previously impeded recovery of pure IELs. First, it dissects away epithelial cells from the intestine without disrupting the basement membrane. This prevents contamination of IEL preparations with lamina propria and Peyer's patch lymphocytes. Second, it eliminates many purification steps that have previously been required. These include incubation in chelating agents, mincing, vigorous shaking, eversion of the intestine, and panning (Lefrançois, 1994). Each of those procedures can cause substantial non-specific cell losses, leading to low cell yields. Previously published isolation protocols yield 5–15 million IELs/rat (Fangmann et al., 1991b; Teitelbaum et al., 1995; Kearsey and Stadnyk, 1996). The IEL population in the rat has, however, been estimated to be 10- to 20-fold larger (Cerf-Bensussan and Guy-Grand, 1991; Kraehenbuhl and Neutra, 1992). The method we have developed routinely yields 30–50 million IELs/rat.

4.2. $\gamma\delta TcR^+$ rat IELs

Consistent with previous reports (Fangmann et al., 1991b), many of the IELs isolated with our procedure were $CD8^+RT6^+\alpha\beta TcR^+$ (Fangmann et al., 1990; Takimoto et al., 1992; Torres-Nagel et al., 1992; Kearsey and Stadnyk, 1997). Few were $CD4^+CD8^+$ or $CD8^-CD4^+$. A major new finding, however, was the identification of a population of $\gamma\delta TcR^+$ IELs that comprise $\sim 25\%$ of total IELs recovered. Previously it has been reported that V65-stained $\gamma\delta TcR^+$ IELs comprise either $< 10\%$ (Kuhnlein et al., 1994; Helgeland et al., 1997; Kearsey and Stadnyk, 1997) or 10–20% (Helgeland et al., 1996; Gorczynski et al., 1996) of the rat IEL population. The percentage of $\gamma\delta TcR^+$ cells has been reported to be 40–50% of the total IEL population in the mouse (Goodman and Lefrançois, 1988), and the present data suggest that the rat IEL population may be more like that of the mouse than previously thought.

It could be argued that the high percentage of $\gamma\delta TcR^+$ IELs we observed reflects a selective loss of $\alpha\beta TcR^+$ IELs due to hypoxic isolation conditions, but we think such an explanation is unlikely.

First, the absolute number of $\alpha\beta TcR^+$ cells that we recovered was higher than that produced by other methods. In addition, analysis of lymphoid cells immediately after the flushing step in our procedure revealed > 90% viability.

We recognize, however, that a number of factors other than isolation methodology could influence $\gamma\delta TcR^+$ IEL percentages. For example, there could be compartmentalization of $\gamma\delta TcR^+$ cells in the gut, and the percentage of these cells could vary along its length. Our procedure isolated IELs from the entire small bowel, and it is possible that previous reports based on the older methodology simply used different regions of the bowel. In a preliminary study, however, we found high percentages of $\gamma\delta TcR^+$ IELs in proximal, middle, and distal small intestine (DT, unpublished observations).

It could also be argued that the proportion of $\gamma\delta TcR^+$ cells in the WF rat IEL compartment may differ from the proportion in rats of other strains or ages. Our analysis of five phenotypically normal strains at $\sim$ 10 weeks of age suggests that, although there is some strain-to-strain variability, the percentage in WF rats is not uniquely high. Whether the percentage is also high in older or younger animals analyzed by our method is not yet established, however.

4.3. Rat IEL sub-populations

Our three-color microfluorometric analysis identified five major sub-populations of IELs based on the expression of CD4, CD8, and TcR. These five major sub-populations were further categorized using additional phenotypic criteria.

One of these five sub-populations, comprising $CD8^-CD4^+\alpha\beta TcR^+$ cells, has previously been interpreted to be indicative of contamination with lamina propria and/or Peyer's patch lymphocytes (Lefrançois, 1994). We believe, however, that this interpretation is not correct. B-lymphocytes are a sensitive measure of contamination of IEL populations with lamina propria and Peyer's patch lymphocytes (Kearsey and Stadnyk, 1996), and we observed very low numbers of B cells in our IEL preparations (Fangmann et al., 1991b; Lefrançois, 1994).

Essentially all of the cells in each of the five major IEL sub-populations expressed the activation marker CD25, suggesting that the intestinal environment activates IELs irrespective of their intestinal or thymic origin. The presence of $CD25^+$ IELs further suggests that IL-2 may be produced in the intestinal tissue and may in part control the functional activity of IELs. This inference is supported by the detection of abundant IL-2 mRNA in preparations of purified IELs (Kearsey and Stadnyk, 1996).

The variable expression of CD5 we observed in the IEL sub-populations has been previously noted, and it has been suggested that the variability is age-related (Fangmann et al., 1991b; Takimoto et al., 1992). Our data suggest that, in addition to age, expression of CD5 may be subset-dependent. Depending on subset, the proportion of $CD5^+$ cells varied from very low to very high (Table 3).

4.4. Intraepithelial NK cells

The present studies have also identified and characterized a population of $\alpha\beta^-$ and $\gamma\delta TcR^-$ IELs that express the NKR-P1 marker; such cells are NK cells (Chambers et al., 1989). This population of cells was almost completely restricted to the $CD4^-CD8^-$ IEL population and are $CD2^-$. They are unlike peripheral NK cells in the rat, which are $CD2^+$ (Vaage et al., 1991) and $CD8^+$ (Woda and Biron, 1986). Cells positive for NKR-P1 staining comprised 25–30% of IELs. The majority of the $NKR-P1^+$ NK cells were also $RT6^+$ and $CD25^+$. In a preliminary report, it has been suggested that peripheral NK cells express low levels of RT6 (Wonigeit et al., 1997), and recent work in our laboratory has confirmed this report (DT, unpublished observations). In contrast, we observed that RT6 is expressed on NK IELs at a very high density that was comparable to that observed on TcR^+ IELs (Fangmann et al., 1991a,b; Waite et al., 1996).

5. Conclusion

In conclusion, we report a new isolation method for rat IELs that is noteworthy for its reproducible high yields. IELs isolated using this method include five major sub-populations, among them significant numbers of $\gamma\delta TcR^+$ and NK cells. The rapidity, efficiency, and product purity that characterize the

method should facilitate functional and developmental studies of IEL sub-populations in the rat. Detailed analysis of IEL sub-populations using this new method may facilitate analyses of the mechanisms of oral tolerance.

Acknowledgements

References

Cerf-Bensussan, N., Guy-Grand, D., 1991. Intestinal intraepithelial lymphocytes. Gastroenterol. Clin. North Am. 20, 549.

Chambers, W.H., Vujanovic, N.L., DeLeo, A.B., Olszowy, M.W., Herberman, R.B., Hiserodt, J.C., 1989. Monoclonal antibody to a triggering structure expressed on rat natural killer cells and adherent lymphokine-activated killer cells. J. Exp. Med. 169, 1373.

Colle, E., Fuks, A., Poussier, P., Edouard, P., Guttmann, R.D., 1992. Polygenic nature of spontaneous diabetes in the rat: Permissive MHC haplotype and presence of the lymphopenic trait of the BB rat are not sufficient to produce susceptibility. Diabetes 41, 1617.

Crisá, L., Greiner, D.L., Mordes, J.P., MacDonald, R.G., Handler, E.S., Czech, M.P., Rossini, A.A., 1990. Biochemical studies of RT6 alloantigens in BB/Wor and normal rats: evidence for intact but unexpressed RT6[a] structural gene in diabetes prone BB rats. Diabetes 39, 1279.

Davies, M.D., Parrott, D.M., 1981. Preparation and purification of lymphocytes from the epithelium and lamina propria of murine small intestine. Gut 22, 481.

Ebert, E.C., Roberts, A.I., 1995. Pitfalls in the characterization of small intestinal lymphocytes. J. Immunol. Meth. 178, 219.

Fangmann, J., Schwinzer, R., Winkler, M., Wonigeit, K., 1990. Expression of RT6 alloantigens and the T cell receptor on intestinal intraepithelial lymphocytes of the rat. Transplant. Proc. 22, 2543.

Fangmann, J., Schwinzer, R., Hedrich, H.-J., Klöting, I., Wonigeit, K., 1991a. Diabetes-prone BB rats express the RT6 alloantigen on intestinal intraepithelial lymphocytes. Eur. J. Immunol. 21, 2011.

Fangmann, J., Schwinzer, R., Wonigeit, K., 1991b. Unusual phenotype of intestinal intraepithelial lymphocytes in the rat: predominance of T cell receptor $\alpha/\beta^+/CD2^-$ cells and high expression of the RT6 alloantigen. Eur. J. Immunol. 21, 753.

Fangmann, J., Schwinzer, R., Hedrich, H.-J., Wonigeit, K., 1993. Demonstration of RT6 expression on a $CD3^-$ population of intestinal intraepithelial lymphocytes of athymic nude rats. Transplant. Proc. 25, 2789.

Goodman, T., Lefrançois, L., 1988. Expression of the gamma-delta T cell receptor on intestinal $CD8^+$ intraepithelial lymphocytes. Nature 333, 855.

Gorczynski, R.M., Chen, Z., Cohen, Z., Plapler, H., Wojcik, D., 1996. Phenotypic and functional assessment of intraepithelial lymphocytes (IEL) isolated from rat colon and small bowel. Immunol. Lett. 50, 131.

Helgeland, L., Vaage, J.T., Rolstad, B., Midtvedt, T., Brandtzaeg, P., 1996. Microbial colonization influences composition and T cell receptor V beta repertoire of intraepithelial lymphocytes in rat intestine. Immunology 89, 494.

Helgeland, L., Vaage, J.T., Rolstad, B., Halstensen, T.S., Midtvedt, T., Brandtzaeg, P., 1997. Regional phenotypic specialization of intraepithelial lymphocytes in the rat intestine does not depend on microbial colonization. Scand. J. Immunol. 46, 349.

Iwakoshi, N.N., Goldschneider, I., Tausche, F., Mordes, J.P., Rossini, A.A., Greiner, D.L., 1998. High frequency apoptosis of recent thymic emigrants in the liver of lymphopenic diabetes prone BioBreeding rats. J. Immunol. 160, 5838.

Kearsey, J.A., Stadnyk, A.W., 1996. Isolation and characterization of highly purified rat intestinal intraepithelial lymphocytes. J. Immunol. Meth. 194, 35.

Kearsey, J.A., Stadnyk, A.W., 1997. Class II MHC expression on rat intestinal intraepithelial lymphocytes. Immunol. Lett. 55, 63.

Kraehenbuhl, J.P., Neutra, M.R., 1992. Molecular and cellular basis of immune protection of mucosal surfaces. Physiol. Rev. 72, 853.

Kuhnlein, P., Park, J.H., Herrmann, T., Elbe, A., Hunig, T., 1994. Identification and characterization of rat gamma/delta T lymphocytes in peripheral lymphoid organs, small intestine, and skin with a monoclonal antibody to a constant determinant of the gamma/delta T cell receptor. J. Immunol. 153, 979.

Kuhnlein, P., Mitnacht, R., Torres-Nagel, N.E., Herrmann, T., Elbe, A., Hunig, T., 1996. The canonical T cell receptor of dendritic epidermal gamma delta T cells is highly conserved between rats and mice. Eur. J. Immunol. 26, 3092.

Lefrançois, L., 1994. Isolation of mouse small intestinal intraepithelial lymphocytes. In: Coligan, J.E., Kruisbeek, A.M., Margulies, D.H., Shevak, E.M., Strober, W. (Eds.), Current Protocols in Immunology. Wiley, New York, p. 19.1.

Lundqvist, C., Hammarstrom, M.L., Athlin, L., Hammarstrom, S., 1992. Isolation of functionally active intraepithelial lympho-

cytes and enterocytes from human small and large intestine. J. Immunol. Meth. 152, 253.

Mayrhofer, G., Whately, R.J., 1983. Granular intraepithelial lymphocytes of the rat small intestine: I. Isolation, presence in T lymphocyte-deficient rats and bone marrow origin. Int. Arch. Allergy Appl. Immunol. 71, 317.

Mosley, R.L., Klein, J.R., 1992. A rapid method for isolating murine intestine intraepithelial lymphocytes with high yield and purity. J. Immunol. Meth. 156, 19.

Sakai, T., Agui, T., Matsumoto, K., 1994. Intestinal intra-epithelial lymphocytes in LEC mutant rats. Immunol. Lett. 41, 185.

Takimoto, H., Nakamura, T., Takeuchi, M., Sumi, Y., Tanaka, T., Nomoto, K., 1992. Age-associated increase in number of $CD4^+CD8^+$ intestinal intraepithelial lymphocytes in rats. Eur. J. Immunol. 22, 159.

Teitelbaum, D.H., Neideck, B., Lee, J., Merion, R.M., 1995. Inhibitory activity of intestinal intraepithelial lymphocytes. Surgery 118, 378.

Teitelbaum, D.H., Del Valle, J., Reyas, B., Post, L., Gupta, A., Mosely, R.L., Merion, R., 1996a. Intestinal intraepithelial lymphocytes influence the production of somatostatin. Surgery 120, 227.

Teitelbaum, D.H., Reyes, B.C., Merion, R.M., Lee, M., 1996b. Intestinal intraepithelial lymphocytes: identification of an inhibitory subpopulation. J. Surg. Res. 63, 123.

Torres-Nagel, N., Kraus, E., Brown, M.H., Tiefenthaler, G., Mitnacht, R., Williams, A.F., Hunig, T., 1992. Differential thymus dependence of rat CD8 isoform expression. Eur. J. Immunol. 22, 2841.

Vaage, J.T., Dissen, E., Ager, A., Fossum, S., Rolstad, B., 1991. Allospecific recognition of hemic cells in vitro by natural killer cells from athymic rats: evidence that allodeterminants coded for by single major histocompatibility complex haplotypes are recognized. Eur. J. Immunol. 21, 2167.

Waite, D.J., Appel, M.C., Handler, E.S., Mordes, J.P., Rossini, A.A., Greiner, D.L., 1996. Ontogeny and immunohistochemical localization of thymus dependent and thymus independent $RT6^+$ cells in the rat. Am. J. Pathol. 148, 2043.

Woda, B.A., Biron, C.A., 1986. Natural killer cell number and function in the spontaneously diabetic BB/W rat. J. Immunol. 137, 1860.

Wonigeit, K., Dinkel, A., Fangmann, J., Thude, H., 1997. Expression of the ectoenzyme RT6 is not restricted to resting peripheral T cells and is differently regulated in normal peripheral T cells, intestinal IEL, and NK cells. Adv. Exp. Med. Biol. 419, 229.

Zadeh, H.H., Greiner, D.L., Wu, D.Y., Tausche, F., Goldschneider, I., 1996. Abnormalities in the export and fate of recent thymic emigrants in diabetes-prone BB/W rats. Autoimmunity 24, 35.